Cellulose IIIICrystal Structure and Hydrogen Bonding by Synchrotron X-ray and Neutron Fiber Diffraction

ARTICLE *in* MACROMOLECULES · NOVEMBER 2004

Impact Factor: 5.8 · DOI: 10.1021/ma0485585

4 AUTHORS, INCLUDING:

Henri Chanzy
French National Centre for Scientific Research
69 PUBLICATIONS **4,733** CITATIONS
SEE PROFILE

Yoshiharu Nishiyama
French National Centre for Scientific Research
100 PUBLICATIONS **6,135** CITATIONS
SEE PROFILE

Paul Langan
Oak Ridge National Laboratory
122 PUBLICATIONS **2,991** CITATIONS
SEE PROFILE

Cellulose III_I Crystal Structure and Hydrogen Bonding by Synchrotron X-ray and Neutron Fiber Diffraction

Masahisa Wada,[†] Henri Chanzy,[‡] Yoshiharu Nishiyama,[‡] and Paul Langan*[,§]

Department of Biomaterials, Graduate School of Agricultural and Life Sciences, The University of Tokyo, Tokyo 113-8657, Japan, Centre de Recherches sur les Macromolécules Végétales−CNRS, affiliated with the Joseph Fourier University of Grenoble, BP 53, 38041 Grenoble Cedex 9, France, and Bioscience Division, Los Alamos National Laboratory, Los Alamos, New Mexico 87545

Received July 15, 2004; Revised Manuscript Received September 2, 2004

ABSTRACT: The crystal and molecular structure, together with the hydrogen-bonding system in ammonia-mercerized cellulose III_I, has been determined using synchrotron X-ray and neutron fiber diffraction data. The structure has a one-chain monoclinic unit cell with an asymmetric unit that contains only one glucosyl residue and with the hydroxymethyl group in the *gt* conformation. The hydrogen-bonding system is well-defined with no evidence of disorder. A bifurcated hydrogen bond links a donating secondary alcohol O3 atom to a ring O5 atom (major) and a primary alcohol O6 atom (minor) of an adjacent residue in the same chain. Two hydrogen bonds are present between neighboring chains, perpendicular to the chain direction. A detailed comparison of the crystal structure and hydrogen-bonding system reported here for cellulose III_I and those reported previously for the other cellulose polymorphs is given. The conformation of the chain in cellulose III_I has features similar to that of the center chain in the highly stable cellulose II allomorph. However, unlike in cellulose II, the chains are parallel, as in cellulose I_α and cellulose I_β.

Introduction

It has been known for close to 70 years that liquid ammonia can penetrate and swell cellulose crystals to yield crystalline cellulose ammonia complexes.[1−5] Following ammonia evaporation, cellulose does not revert to its initial crystal form but adopts another, designated cellulose III. Cellulose III obtained from decomplexation of ammonia−cellulose I or ammonia−cellulose II is designated cellulose III_I or cellulose III_{II}, respectively. Early X-ray fiber diffraction studies by the group of Sarko suggest that cellulose III_I and cellulose III_{II} have the same unit cell (space group $P2_1$; $a = 10.25$ Å, $b = 7.78$ Å, $c = 10.34$ Å, $\gamma = 122.4°$) containing two chains but that the chains are parallel in cellulose III_I and antiparallel in cellulose III_{II}.[6] Cellulose III is metastable, reverting to its parent form on hydrothermal treatment; cellulose I from cellulose III_I and cellulose II from cellulose III_{II}. The preparation of cellulose III is not limited to the action of liquid ammonia; a number of mono-, di-, and triamines give crystalline cellulose−amine complexes that yield cellulose III upon washing in nonaqueous solvents.[7−11]

Treatment with ammonia or amines is a simple way to increase the accessibility of crystalline cellulose and also to increase its reactivity when preparing cellulose derivatives.[3,8,12−14] A number of industrial applications in the fields of textile, pulp and paper, and cellulose derivatives are based on the specific properties of materials having the cellulose III structure. In addition to enhanced accessibility and chemical reactivity, these products have increased softness and plasticity.[15−19]

Although few details exist on the structure of cellulose III_{II},[20] the conversion of cellulose I to cellulose III_I has been studied at both structural and ultrastructural levels.[21−23] Unlike mercerization, individual microfibrils survive conversion from cellulose I to cellulose III_I, although in a changed form. Each microfibril becomes inflated under the penetration of ammonia or amine molecules. After evaporating or washing away the guest molecules, the microfibrils look deflated and crumpled, have convoluted sections, have increased specific surfaces, and are substantially decrystallized.[22−25]

At the molecular level, a comparison of ^{13}C CP/MAS NMR spectra indicates that the conformation of the chains in cellulose III_I differs from that of cellulose I.[26−29] Spectra from cellulose I can be complicated because of contributions from two naturally occurring allomorphs, cellulose I_α and cellulose I_β, and also because each allomorph has two conformationally distinct glucosyl residues. In general, the signals from each C atom occur as multiplets and singlets in spectra from cellulose I and from cellulose III_I, respectively. In addition, the chemical shifts of the C6 atoms are significantly different: 62 ppm for cellulose III_I as opposed to 65 ppm for cellulose I.[26−29] This last observation can be correlated to the hydroxymethyl moieties rotating from their *tg* conformation in cellulose I to the *gt* conformation in cellulose III_I.[30,31] Such a rotation, related to complex formation during the penetration of the guest molecules,[32,33] has been proposed to act as a barrier to cellulose I recovery at room temperature.

The early structural study of cellulose III_I by Sarko's group[6] was based on the measurement of 23 X-ray reflections. In the resulting structure, the two chains in the unit cell are independent, parallel to one another, and located on 2-fold screw axes. Thus, the unit cell is generated from an asymmetric unit that contains two independent glucosyl units. The hydroxymethyl groups of both chains are close to the *tg* conformation. However, the solid-state NMR data do not support these features. The occurrence of only six resonances for cellulose III_I is in favor of a crystal structure in which the asymmetric

[†] The University of Tokyo.
[‡] Joseph Fourier University of Grenoble.
[§] Los Alamos National Laboratory.
* Corresponding author: e-mail langan_paul@lanl.gov; Tel 505 665 8125; Fax 505 665 3024.

10.1021/ma0485585 CCC: $27.50
Published on Web 10/22/2004

unit contains one glucosyl residue, not two. The occurrence of the C6 resonance at around 62 ppm for cellulose III_I indicates that the hydroxymethyl group is in the *gt* conformation, not the *tg* conformation.

The present work is devoted to a revision of the structure of cellulose III_I. We have used improved methods to prepare highly crystalline fibers of cellulose III_I, using supercritical ammonia treatments,[28,34,35] that diffract synchrotron X-rays to atomic resolution,[28] allowing the precise location of C and O atoms. A method has also been devised, using deuterated reagents, for replacing all H atoms involved in hydrogen bonding by D atoms so that their positions can be determined using neutron diffraction. Comparison of the crystal structure and hydrogen-bonding arrangement for cellulose III_I presented here, with those previously determined for cellulose I_α, cellulose I_β, and cellulose II, reveals insights into the factors that determine the structure of cellulose.

Experimental Section

Preparation of Oriented Cellulose I Samples. Green *Cladophora* seaweeds were collected from the Chikura sea, Chiba, Japan. After removing calcite by boiling in 0.1 N HCl, the cellulosic algal cell walls were further purified by repeated treatments with a 5% KOH solution at room temperature followed by a 0.3% $NaClO_2$ aqueous solution at 70 °C.[36] The purified samples were then hydrolyzed into cellulose microcrystals by a sulfuric acid treatment. Oriented thin films consisting of parallel arrays of these microcrystals were prepared according to the method of Nishiyama et al.[37] and then stacked parallel to one another in order to obtain sample sizes large enough for diffraction studies. The stacks were trimmed with a sharp blade to about 100 μm × 200 μm × 10 mm for the X-ray experiments and to about 5 mm × 5 mm × 10 mm for the neutron experiments, the longest dimension corresponding to the long axis of the cellulose microcrystals. Preliminary X-ray studies showed these samples to consist of highly crystalline and oriented composites of cellulose I_α and cellulose I_β.

Conversion into Cellulose III_I. Samples were inserted into a steel pressure vessel, which was cooled in a dry ice/methanol bath. Ammonia (NH_3) gas was slowly introduced until the samples were completely immersed in liquified ammonia. The vessel was then sealed, kept at room temperature for 30 min, and then heated in an oil bath to 140 °C (a few degrees above the critical temperature of ammonia at 132.5 °C). After maintaining this temperature for 1 h, the vessel was removed from the oil bath, and the ammonia gas was allowed to leak out.[28,34] The treated samples were then washed with methanol and vacuum-dried at 50 °C. The same procedure was also used to prepare deuterated cellulose III_I samples, except that deuterated ammonia (ND_3) and deuterated methanol (CH_3OD) were used instead of their hydrogenous counterparts.

Data Collection and Intensity Measurement. X-ray diffraction data were collected at beamline ID2A at the European Synchrotron Radiation Source, Grenoble, France, using an image plate MAR345 with a specimen-to-detector distance of 175 mm and using a wavelength of 0.7208 Å. Preliminary data collection indicated that the samples are not truly symmetric about the fiber axis but textured. A data collection strategy previously developed for textured cellulose samples was therefore used.[38] This strategy involved mounting the specimen with its fiber axis parallel to the φ axis of the goniometer and then collecting a series of diffraction diagrams at 15° intervals in φ. In addition, diffraction diagrams were collected with the fiber axis progressively titled in steps of 2° in order to record missing reflections close to the meridian. A typical X-ray diagram is shown in Figure 1a (top).

Neutron diffraction data were collected at D19 at the Institut Laue Langevin, Grenoble, France, from both hydrogenated and deuterated specimens. The data collection strategy was different from that employed with X-rays because of the need to step the detector and also because, given that the texture information had already been recorded in the X-ray experiment, only data from a plane perpendicular to the film surface in reciprocal space were required. Typical neutron fiber diffraction diagrams of the hydrogenated and deuterated samples are shown in Figure 1b (top). The background, mostly due to incoherent scattering from hydrogen, was evaluated and removed following the method of von der Linden et al.,[39] extended in two dimensions. Corrections for sample volume and attenuation effects were obtained by flattening the background. A summary of the experimental parameters is given in Table 1.

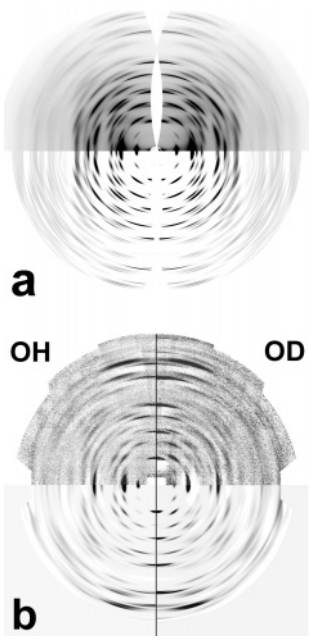

Figure 1. (a) Top: synchrotron X-ray diffraction data collected on an on-line MAR image plate from an oriented sample of cellulose III_I on station ID2A at the ESRF, Grenoble France. Bottom: a fit of the top pattern obtained during the measurement of the Bragg intensities and background using software that takes into account fiber texture.[40] Comparison of the top and bottom of (a) indicates the agreement between observed and measured Bragg intensities. **(b)** Top: neutron fiber diffraction patterns collected from oriented samples of cellulose III_I, one hydrogenated (left-hand quadrant) and the other deuterated (right-hand quadrant). The bottom quadrants show 3D fits of the Bragg intensities using software that takes into account fiber texture.[41] The images in **(a)** and **(b)** have been remapped into cylindrical reciprocal space with the fiber axis vertical.

The diffraction intensities were obtained by fitting the diagrams, using the fiber axis orientation obtained from a pole figure of the (004) reflection, as described previously.[40] The reflections (100) and ($1\bar{1}0$) have similar *d*-spacings in cellulose III_I and were therefore treated as composite. The X-ray intensity ratio of this composite varied with rotation around the fiber axis by about ±30%. Whereas in previous texture measurements with cellulose I two independent intensity ratios could be measured,[38] only one was available for cellulose III_I, and an exact orientation distribution could not be measured. Instead, a sinusoidal orientation distribution function was assumed as a first approximation. The intensity ratio fluctuation was within 5% after correction.

Structure Refinement. X-ray structure refinement was carried out using previously described strategies for applying SHELX-97[41] to high-resolution fiber diffraction data.[42] Atomic starting positions were taken from the average chain conformation in the crystal structure of cellulose I_β.[38] An initial refinement was carried out with the hydroxymethyl group O atom removed and the chains arranged in the "parallel-up"[43]

Table 1. Experimental Details

	X-ray	neutron
crystal data		
chemical formula	$C_{12}H_{20}O_{10}$	$C_{12}H_{14}D_6O_{10}$
cell setting, space group	monoclinic, $P2_1$	monoclinic, $P2_1$
a (Å)	4.450(4)	4.450(4)
b (Å)	7.850(8)	7.850(8)
c (Å)	10.310(10)	10.310(10)
α (deg)	90	90
β (deg)	90	90
γ (deg)	105.10(5)	105.10(5)
V (Å^3)	347.7(6)	347.7(6)
Z	1	1
crystalline density	1.54	
radiation type	synchrotron X-ray	neutron
λ (Å)	0.72060	1.30580
data collection		
diffractometer	ID2A	D19
independent reflections	137	74
reflections $>2\sigma(I)$	113	55
θ_{max} (deg)	19.93	32.95
range of h	$0 \rightarrow 4$	$0 \rightarrow 3$
range of k	$-6 \rightarrow 7$	$-6 \rightarrow 5$
range of l	$-9 \rightarrow 9$	$-8 \rightarrow 8$
refinement		
refinement on	F^2	F^2
$R[F^2 > 2\sigma(F^2)]$	0.1777	0.2178
$\omega R(F^2)$	0.3876	0.5000
$\Delta\rho_{max}$	0.284	1.177
$\Delta\rho_{min}$	−0.338	−1.028
ρ_{rms}	0.087	0.325

configuration. The orientation of the chains was free to refine. The corresponding calculated Omit map showed no sign of hydroxymethyl group disorder and clearly indicated that this group was in the gt[30] conformation (Figure 2). The subsequent refinement of all atomic positions, with the exception of H atoms on hydroxyl groups, with global scaling and thermal parameters involved a total of 35 parameters and 43 restraints and resulted in values of 17.77% and 38.76% for R and $R\omega$, respectively.[44]

Allowing individual thermal parameters to refine involved eight additional parameters and resulted in values of 17.64% and 38.15% for R and $R\omega$, respectively. A statistical significance test[45] based on the ratio of the values of $R\omega$ indicates that this improvement is significant only at a 75% confidence

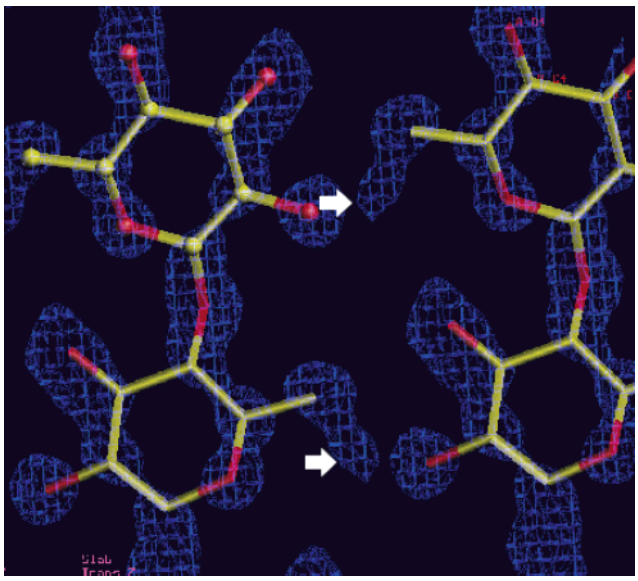

Figure 2. Section through an Omit map calculated using the observed X-ray amplitudes and model phases but omitting the hydroxymethyl group O atom from the phase calculation. The skeletal model represents the cellulose chain. Density (indicated by arrows) can be clearly associated with the hydroxymethyl group in the gt position.

Table 2. Fractional Atomic Coordinates of the Atoms for One Glucosyl Residue of the Chain of Cellulose III$_I$[a]

atom	x	y	z
C1	0.050961	0.057262	0.380527
C2	0.191389	0.196135	0.287129
C3	0.047193	0.160362	0.153425
C4	0.009263	−0.031267	0.112801
C5	−0.148745	−0.157932	0.218384
C6	−0.176129	−0.348168	0.188882
O2	0.181636	0.366971	0.331722
O3	0.242720	0.281823	0.066537
O4	−0.191038	−0.076143	0.000711
O5	0.038639	−0.114787	0.333349
O6	−0.238242	−0.451795	0.303957
H1	−0.164524	0.062564	0.393673
H2	0.411219	0.197152	0.278760
H3	−0.158495	0.183912	0.154995
H4	0.213656	−0.050262	0.093348
H5	−0.356184	−0.141547	0.235149
H6A	−0.342927	−0.390800	0.126975
H6B	0.016046	−0.359921	0.150091
oH2	0.40(2)	0.442(16)	0.33(3)
oH3	0.15(4)	0.27(3)	−0.020(8)
oH6	−0.12(6)	−0.54(3)	0.30(2)

[a] The hydroxyl hydrogen atom positions oH2, oH3, and oH3 correspond to the deuterons D2, D3, and D6 in the text.

level, and we therefore did not consider the refinement with individual thermal parameters further. A refinement in which the chains were arranged in the "parallel-down" configuration resulted in values of 25.59% and 53.40% for R and $R\omega$, respectively, and could be rejected with respect to the "parallel-up" refinement at a 99.5% level of confidence. The coordinates of the final model are given in Table 2.

Neutron difference amplitudes, $F_d - F_h$, were combined with the phases calculated from the X-ray structure in a Fourier difference synthesis, where F_d and F_h correspond to amplitudes collected from the deuterated and hydrogenous samples, respectively. Labile deuterons on hydroxyl groups were identified with difference density peaks in the synthesis, and their positions were subsequently refined using SHELX-97 and previously described strategies.[38,46,47] The resulting values for R and $R\omega$ were 0.218 and 0.500. Allowing the occupancy of the D atom positions to refine did not significantly improve the agreement with the data.

The deuteron associated with the primary alcohol O3 atom, D3, refined to a position that unambiguously indicates that it is donated to the ring oxygen O5 atom and the secondary alcohol O6 atom of an adjacent sugar residue in the same chain. The atom labels are as in Nishiyama et al.[38] The deuterons associated with the O2 and O6 atoms, D2 and D6, refined to positions that indicate they are donated to O6 and O2 atoms on neighboring chains, respectively, in a donor and acceptor arrangement designated A. The alternative donor and acceptor assignment for these hydrogen bonds, designated B, can be obtained by rotation of the hydroxyl groups in question. The net effect of these rotations is a displacement of D atoms by only ∼0.6 Å along the O2···O6 hydrogen bond directions. A structure refined with assignment B resulted in values of 0.219 and 0.523 for R and $R\omega$. The refinement with assignment B can only be rejected with respect to the refinement with assignment A at a confidence level of 90%. To test for disorder, both A and B assignments were incorporated into the same structure, by associating two partial D2 and D6, atoms with each O2 and O6 atom. The total occupancy associated with each hydrogen bond was constrained to unity. Each deuteron was given an initial occupancy of 0.5. The deuterons in arrangements A and B refined to occupancies of 0.64 and 0.36, respectively, with resultant values of 0.207 and 0.488 for R and $R\omega$. This refinement is an improvement with respect to the structure with assignment A only at a confidence level of 75%, and we therefore did not consider this refinement further. The refined coordinates of the hydrogen atoms in A are given in Table 2. The hydrogen-bonding parameters are given in Table 3.

Table 3. Hydrogen Bonds with H···A < *R* (Å) + 2.000 Å and ∠DHA > 110°[a]

D−H	*d*(D−H)	*d*(H···A)	∠DHA	*d*(D···A)	A	
O2−oH2	0.981	1.642	173	2.619	O6	$[x+1, y+1, z]$
O3−oH3	0.982	1.979	149	2.866	O5	$[-x, -y, z-1/2]$
O3−oH3	0.987	2.281	131	3.021	O6	$[-x, -y, z-1/2]$
O6−oH6	0.996	1.706	159	2.642	O2	$[x, y-1, z]$

[a] The hydroxyl hydrogen atom positions oH2, oH3, and oH3 correspond to the deuterons D2, D3, and D6 in the text.

Table 4. Selected Conformational Parameters of Cellulose III_I Compared with Those of the Other Cellulose Allomorphs[a]

	Φ	Ψ	τ	χ	χ′	θ
cellulose III_I	−92	93	116	44	163	10.5
cellulose II origin[43]	−97	95	116	72	−165	5.0
cellulose II center[43]	−94	87	115	58	−175	10.2
cellulose I_α up[48]	−99	95	116	166	−74	6.9
cellulose I_α down[48]	−98	99	116	167	−75	9.4
cellulose I_β origin[39]	−98	90	115	170	−70	10.2
cellulose I_β center[39]	−89	94	116	158	−83	6.7

[a] The conformation of the hydroxymethyl group is defined by two letters, the first referring to the torsion angle χ (O5−C5−C6−O6) and the second to the torsion angle χ′ (C4−C5−C6−O6). Thus, the ideal *tg* and *gt* conformations would be respectively be defined as sets of two angles (180°, 60°) and (60°, 180°). The glycosidic bond angle τ is defined by (C1−O4−C4). The glycosidic torsion angles Φ and Ψ, which describe the relative orientation of adjacent glucosyl residues in the same chain, are defined by (O5−C1−O1−C4) and (C1−O1−C4−C3), respectively.

Results and Discussion

The unit cell dimensions reported here agree with those recently reported by Wada et al.[28] and correspond to a one chain unit cell, in contrast to the two chain unit cell reported previously by Sarko et al.[6] The $P2_1$ space group of cellulose III_I has an asymmetric unit that contains only one glucosyl residue, whereas the asymmetric units of all other cellulose allomorphs we have previously studied using X-ray and neutron diffraction (cellulose II,[42,46] cellulose I_α,[47] and cellulose I_β[38]) contain two glucosyl residues.

In the much smaller X-ray data set recorded by Sarko et al. from cellulose III_I prepared from ramie fibers,[6] reflections are present that do not appear in the more extensive data set reported here and that rule out a one chain unit cell. This may be due to an incomplete conversion of cellulose I to cellulose III_I. Another possibility is that conversions of ramie and algal samples result in two distinct crystal forms of cellulose III_I. However, this seems unlikely given that the solid-state ^{13}C NMR spectra of cellulose III_I prepared from ramie and algal celluloses are identical.[27]

A comparison of selected conformational features of cellulose III_I and the other cellulose allomorphs is given in Table 4. The relative orientation of adjacent glucosyl residues can be described by the glycosidic torsion angles Φ and Ψ and the bond angle τ, and the conformation of hydroxymethyl groups can be described by torsion angles χ and χ′.[30] The values of the parameters in Table 4 are all well within the ranges observed in crystals of small analogues of cellulose[48−52] as well as those of the other cellulose allomorphs.[38,42,46,47]

The conformation of the glycosidic linkage is closest to those found in cellulose II. The conformation of the sugar ring has a relatively large value of 10.5 for the Cremer and Pople puckering parameter, θ.[53] A similarly large value of 10.2 is observed for θ in the center chain of cellulose II. However, these values are not unusual for β-glucose rings and therefore do not indicate a large amount of strain.[52] The similarity between the conformation of the chain in cellulose III_I and the center chain of cellulose II supports the observation made by Wada et al.[28] that the ^{13}C CP/MAS NMR spectrum of cellulose III_I is similar to a subset of the spectrum of cellulose II.

The conformation of the hydroxymethyl groups in cellulose III_I is *gt*, as in cellulose II and unlike in cellulose I_α and cellulose I_β where their conformation is *tg*. This is in good agreement with the value of 62.3 ppm[28] observed for the C6 chemical shift in the ^{13}C solid-state NMR spectrum of cellulose III_I, a value within the range given by Horii et al.[31] for the occurrence of the *gt* conformation in sugar hydroxymethyl groups. In the two-chain cellulose III_I structure of Sarko et al.,[6] the hydroxymethyl groups of both chains are near the *tg* conformation. A C6 resonance has never been reported for cellulose III_I in the region of 65 ppm associated with the *tg* conformation.[31] In the present work, the location of the hydroxymethyl group in the OMIT map in Figure 2 unambiguously confirms that the *gt* conformation is correct.

As in cellulose II, cellulose I_α, and cellulose I_β there is an O3−H···O5 intrachain chain hydrogen bond (Figure 3). In cellulose II and cellulose III_I, because of the *gt* conformation of the hydroxymethyl group, this hydrogen bond is bifurcated with a major component, O3−H···O5, and a minor component, O3−H···O6, the major and minor components being classified as moderate and weak, respectively, according to the definition given by Jeffrey.[54] Whereas in cellulose II the major and minor components have average donor acceptor distances of 2.7 and 3.26 Å, respectively, they are 2.87 and 3.02 Å in cellulose III_I, indicating a more even bifurcation. In both cellulose II and cellulose III_I the bifurcated O3−H···O5/O6 hydrogen bond alternates from one side of the chain to the other from glucosyl residue to glucosyl residue along the chain (Figure 3). In cellulose I_α and cellulose I_β, because of the *tg* conformation of the hydroxymethyl group, there is a second intrachain hydrogen bond between O6 and O2 atoms of adjacent residues. This second hydrogen bond restricts the chain conformation, a restriction that may be responsible for the observed disorder between donor and acceptor roles of the O6 and O2 atoms in these allomorphs. In cellulose III_I the chain is not constrained in this way and has more flexibility to adopt a conformation that allows hydrogen bonding without disorder. In cellulose II, this is perhaps also true; however, the cellulose II we have examined so far contained amounts of hydroxymethyl group disorder that confuse the issue.

Using a statistic significance test,[45] we can differentiate between the two possible donor acceptor assignments for the O2···O6 hydrogen bonds in cellulose III_I, A and B, refined against the neutron data only at a confidence level of 90%. This is not a high level of confidence. We cannot say that our inability to more definitively differentiate between these two possibilities is due to the presence of a mixture of these two assignments because a refinement incorporating such disorder is an improvement only at a 75% level of confidence. The most likely reason is that the neutron data collected in this study are less extensive and of lower resolution than those collected previously from cellulose I_α and cellulose I_β because the cellulose III_I samples were less crystalline (158, 216, and 74 neutron

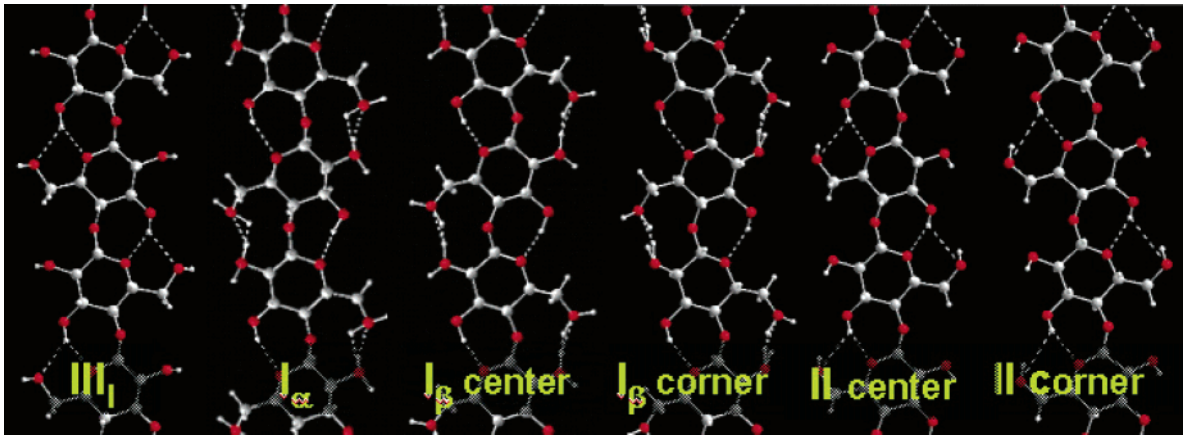

Figure 3. Intrachain hydrogen bonding observed in cellulose III_I, cellulose I_α,[47] cellulose I_β,[38] and cellulose II.[46] C, O, and H atoms are represented by gray, red, and white balls, respectively. Covalent and hydrogen bonds are represented as full and dashed lines, respectively. Disordered hydrogen positions are superimposed in cellulose I_α and cellulose I_β.

intensities extending to 1, 1, and 1.2 Å were used, respectively, in the refinements of cellulose I_α, cellulose I_β, and cellulose III_I). In summary, we can say that the neutron data favor assignment A and that there is no clear evidence for disorder in the hydrogen bonding.

The geometries of the O2···O6 hydrogen bonds in assignment A are more linear and therefore more energetically preferable than in B (the O2···O6 hydrogen bond angles are 159° and 173° for A and 143° and 173° for B). However, this is not a strong argument in support of assignment A because it does not take into account potentially large contributions from dipole−dipole interactions between neighboring hydrogen bonds. It is interesting to note that although the O6−D6···O2 hydrogen bond in assignment A could adopt an almost linear D−H···A angle of 179°, the refined value is only 159°. When the D6 atom is forced into the more linear position, the values of R and $R\omega$ increase. When the D6 atom is released from this constraint, it returns to its previous position.

The lack of evidence for disorder in the hydrogen-bonding system of cellulose III_I may be correlated to differences in the polarized infrared spectrum recorded from this allomorph and those recorded from cellulose I_α and I_β. In the cellulose III_I spectra there is an O−H stretching band of extreme sharpness at 3481 cm^{-1},[28] parallel to the chain direction. This feature is unique among cellulose allomorphs where O−H stretching bands, parallel or perpendicular to the chain axes, are systematically broader. Although it is difficult to fully account for the unusual sharpness of this band, it may be related to the fact that in cellulose III_I there is only one type of intramolecular hydrogen bond per chain, bifurcated O3···O5/O6, whereas in cellulose I_α and I_β there are two, O3···O5 and O6···O2, and the O6···O2 hydrogen bond is disordered. In addition, cellulose I_α, I_β, and II have two independent glucosyl residues, each possessing slightly different O3−H···O5 hydrogen-bonding geometries, complicating the corresponding resonances in the O−H stretching region, whereas cellulose III_I has only one independent glucosyl residue.

The sharpness of the parallel O−H stretching band in cellulose III_I could also be related to the fact that the donor O3 atom in the parallel O3−H···O5 hydrogen bond does not accept any hydrogen bond. According to the classical work of Jakobsen et al.,[55] the breadth of the O−H stretching vibrations in solid alcohols is due mainly to coupling of the vibrations of adjacent O−H groups along chains of hydrogen bonds. The relative widths of the O−H stretching bands of the cellulose allomorphs point to the absence of this coupling in the chain direction of cellulose III_I and its presence in the chain directions of the other cellulose allomorphs. In cellulose I_α and cellulose I_β the donor O3 atoms of the parallel O3−H···O5 hydrogen bond can accept a hydrogen bond from the O6 atom of an adjacent chain. The O6 atoms are involved in disordered hydrogen bond networks that can extend along the length of the microfibril.[56] The intrachain O3−H···O5 stretching vibrations will therefore be coupled in cellulose I_α and I_β and uncoupled in cellulose III_I to those of other hydrogen bonds.

Figure 4 shows projections of the crystal structures of cellulose III_I, cellulose II, cellulose I_α and cellulose I_β down the chain axes. In cellulose I_α and I_β the chains are arranged edge to edge in flat hydrogen-bonded sheets that stack on top of one another in a manner that allows only the atoms at the edge of each sugar ring (in particular, the O6 of the hydroxymethyl group) to significantly overlap with the sugar rings in a neighboring stacked sheet. There are a number of weak C−H··· O intersheet interactions but no intersheet strong O−H···O hydrogen bonds.

In cellulose III_I and cellulose II, the chains lie on top of each other with the sugar rings stacking "like pennies". The stacks are staggered by half a stacking repeat so that each chain can hydrogen bond to two chains in each neighboring stack through strong hydrogen bonds. Chains do not hydrogen bond with other chains in the same stack. A number of different corrugated sheets can be traced that are held together through interchain hydrogen bonds. We can consider cellulose III_I as consisting of identical corrugated sheets of O2−H···O6 hydrogen-bonded chains stacked through O6−H···O2 intersheet hydrogen bonds or, alternatively, as consisting of identical corrugated sheets of O6−H··· O2 hydrogen-bonded chains stacked through O2−H··· O6 intersheet hydrogen bonds. The two different interchain hydrogen bonds lie perpendicular to the chain axes and approximately perpendicular to each other (Figures 4 and 5).

Cellulose II can be considered as consisting of corrugated sheets of parallel chains with all O2−H···O6 or all O6−H···O2 hydrogen bonds in an alternating fashion. The two O2···O6 hydrogen bonds lie perpendicular to the chain axis but approximately parallel to

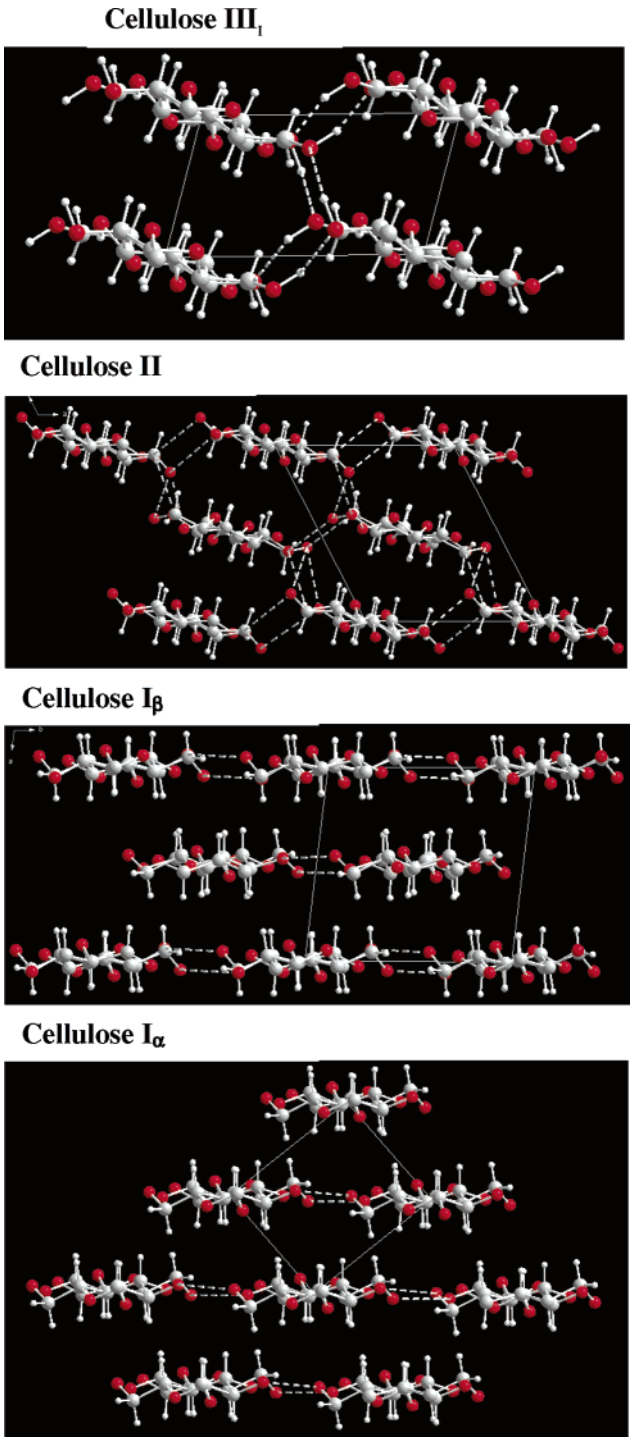

Figure 4. Projections of the crystal structures of cellulose III_I, cellulose II, cellulose I_β, and cellulose I_α down the chain axes directions. C, O, and H atoms are represented as gray, red, and white balls, respectively. Covalent and hydrogen bonds are represented as full and dashed sticks, respectively. H atoms involved in hydrogen bonding are explicitly represented for only cellulose III_I. Only the major components of hydrogen bonds are represented.

each other. The sheets interact through a third type of hydrogen bond, absent from cellulose III_I, between O6 atoms of antiparallel chains. This hydrogen bond is perpendicular to the chain axis and perpendicular to the O2···O6 hydrogen bonds. The main qualitative difference between the hydrogen-bonding arrangements in cellulose II and cellulose III_I would therefore appear to be the presence of a third type of interchain hydrogen

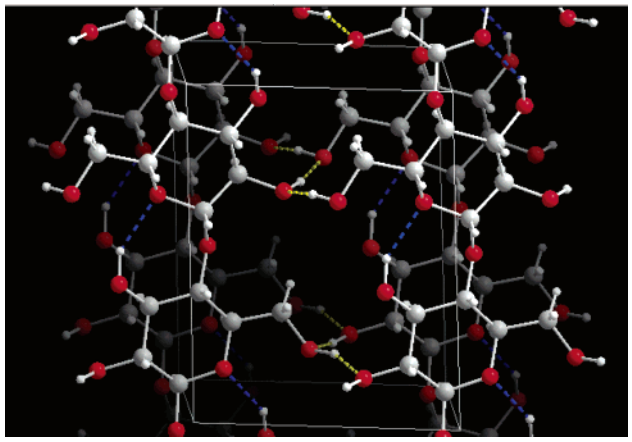

Figure 5. Unit cell of cellulose III_I viewed perpendicular to the *c* axis direction (the chain direction), with the *c* axis tilted slightly to show the zigzag network of interchain O2−H···O6 and O6−H···O2 hydrogen bonds (yellow dashed lines) and the intrachain O3−H···O5 hydrogen bonds (blue dashed lines). The C, O, and H atoms are represented by gray, red, and white balls, respectively. Covalent bonds are represented by full lines. The unit cell is represented by a thin white line.

bond between hydroxymethyl groups of antiparallel chains in cellulose II. This difference can only occur because the chains are parallel in cellulose III_I and antiparallel and staggered in the chain direction in cellulose II.

Rather than considering cellulose III_I and cellulose II as corrugated sheets, another view is to consider the motif as stacks of hydrophobically packed chains connected by infinite chains of cooperative hydrogen bonds. The chains consist of zigzag alternating O2−H···O6 and O6−H···O2 hydrogen bonds in cellulose III_I (Figure 5) and zigzag alternating O2−H···O6, O6−H···O6, and O6−H···O2 hydrogen bonds in cellulose II. This type of hydrogen-bonding arrangement will be particularly strong because of its cooperative nature.

As already mentioned, the sugar rings in cellulose I_α and cellulose I_β are arranged edge to edge in flat sheets, whereas in cellulose III_I the sheets are corrugated. For example, in the case of cellulose I_β when a plane is fitted using least squares to the sugar ring atoms O5, C1, C2, C3 of the origin and center chains, the angle made to the *b* axis direction connecting neighboring chains in a sheet is 2.3(10)° for the origin sheet and 1.9(10)° for the center sheet. In cellulose III_I the angle made by this plane to the *b* axis is 20.2(10)°. The change in chain orientation going from cellulose I_β to cellulose III_I reduces the distance between neighboring chains in a sheet (from 8.20 to 7.85 Å) and increases the separation of sheets (from 3.87 to 4.29 Å). There is a corresponding reduction in density from 1.63 to 1.57. Rotation of the hydroxymethyl group from *tg* in cellulose I_β to *gt* in cellulose III_I has the effect of replacing one of the intrachain hydrogen bonds with an intersheet hydrogen bond. There is no change in the number of intrasheet hydrogen bonds, although there is a change from disorder to order. Another difference is that in cellulose I_β there are a number of weak intersheet C−H···O hydrogen bonds (identified using the criteria D···A < r(D) + r(A) + 0.50 Å, H···A < r(H) + r(A) − 0.12 Å, D−H···A > 100.0°) whereas in cellulose III_I there are none.

From the above discussion, an important difference between cellulose I_β and cellulose III_I is that in cellulose I_β the sheets are tightly packed together, stacking

through relatively hydrophobic weak electrostatic C−H···O hydrogen bonds and van der Waals interactions, whereas in cellulose III_I the sheets are less tightly packed together, stacking through relatively strong O−H···O hydrogen bonds. Both the difference in sheet separation and the nature of the intersheet stacking interactions may contribute to the enhanced accessibility of cellulose III_I for polar guest molecules.

The occurrence of a low-density, thermodynamically unstable crystalline form of cellulose is remarkable in itself and perhaps can only be fully understood by examining its precursor crystalline ammonia−cellulose complex. No X-ray structure of such a complex has been reported to date, but there is structural information on the related crystalline ethylenediamine (EDA)−cellulose complexes.[32] Upon removal of EDA, these complexes also lead to cellulose III_I. Both X-ray data[32] and solid-state NMR data[33,57] indicate that the guest EDA molecules induce a rotation of the hydroxymethyl group from the *tg* to the *gt* conformation. In addition, the cellulose chains in the complex are no longer staggered by one-quarter of the unit cell along the chain axis direction, as in cellulose I_α and cellulose I_β, but are at the same level.[32] The work presented here shows that these features persist in cellulose III_I after the guest molecules have been removed under mild conditions; room temperature evaporation in the case of ammonia and washing with methanol in the case of EDA.

It can be deduced that the removal of guest molecules under mild conditions involves breaking hydrogen bonds between cellulose chains and guest molecules, followed by the establishment of hydrogen bonds between cellulose chains. During this process, the cellulose structure settles into a local pseudo minimum energy that can accommodate the *gt* conformation of the hydroxymethyl groups and that does not involve chain staggering. The metastable character of cellulose III_I is reflected in its density of 1.57 compared to 1.63 for cellulose I_β and 1.61 for cellulose I_α. Only when enough energy is available, for example in hydrothermal treatment, can the chains slide past one another to revert to the quarter staggering arrangement of cellulose I_β, with the concomitant rotation of the hydroxymethyl group from *gt* to *tg*. When cellulose III_I reverts to cellulose I, we have found it always to adopt the cellulose I_β form, even if the initial specimen is rich in cellulose I_α.[26] Cellulose I_β appears to be the most stable and the lowest energy crystal form for cellulose with parallel chains.

It is unclear to us what prevents chain slippage when guest molecules are removed under mild conditions from cellulose III_I. One explanation is that a rotational barrier prevents the hydroxymethyl groups from leaving the *gt* conformation and that this conformation prevents easy slippage of sheets of chains with respect to each other. In this scenario, only when this rotational barrier is overcome during hydrothermal treatment, and the hydroxymethyl group has rotated to the *tg* conformation, can the chains slip. Another explanation is that the positions of the chains are constrained by guest molecules until all of the guest molecules have been removed. In this scenario, hydrogen bonds are established in increasing numbers between constrained chains, and when all guest molecules have been removed, these interchain hydrogen bonds present an energy barrier to chain slippage. Hydrothermal treatment allows these hydrogen bonds to be broken and the chains to slide past one another. In the first scenario, the rotational dynamics of the hydroxymethyl group play a crucial role in the formation of cellulose III_I, whereas in the second, hydrogen bonds established between constrained sheets are more important. Either way, swelling during hydrothermal treatment may play a role by allowing freer rotation of the hydroxymethyl groups as well as disrupting the hydrogen bonds through hydration.

If the solid-state conversion of cellulose I to cellulose III_I is reversible at the crystallographic level, it is certainly not so at the molecular and morphological level. The conversion to cellulose III_I dramatically decreases crystallinity and crystallite size.[21,23,24,58] After reconversion to cellulose I, the crystallinity is poorer than that of the initial sample. [26] A decrease in crystallinity explains to some extent why cellulose III_I and cellulose I reconverted from cellulose III_I have increased accessibility and reactivity toward external agents. Heat annealing can lead to superior crystalline properties with many synthetic polymers. However, the algal cellulose used here is biogenerated with a high degree of crystal perfection, and subsequent treatments do not improve but only degrade the perfection of its native crystalline architecture.

The structure of cellulose III_I presented here, and the possible mechanisms for conversion between cellulose I and cellulose III_I discussed above, raise some interesting questions with regard to what the structure of cellulose III_{II} might be. Solid-state ^{13}C NMR spectra recorded from cellulose III_I and cellulose III_{II} indicate that both phases have hydroxymethyl groups oriented in the *gt* conformation.[27] The initial crystal from of cellulose III_{II} before conversion, cellulose II, also has hydroxymethyl groups in the *gt* conformation.[42,46] Conversion of cellulose II to cellulose III_{II} therefore does not require a large change in hydroxymethyl group orientation, although, as in the conversion of cellulose I to cellulose III_I, it may involve chain slippage and the reorientation of chains. X-ray and neutron fiber diffraction data have been collected from cellulose III_{II}, and structure determination is underway.

Acknowledgment. The authors thank K. Mazeau for valuable discussions and help with molecular displays.The authors also thank the Institut Laue Lagnevin and the European Synchrotron Radiation Facility for the provision of beam time. Y.N. thanks the French Government and the Japanese Society for the Promotion of Science for financial support. P.L. thanks the Office of Science and the Office of Biological and Environmental Research for of the U.S. Department of Energy for financial support.

References and Notes

(1) Hess, K.; Trogus, C. *Ber.* **1935**, *B68*, 1986−1988.
(2) Barry, A. J.; Peterson, F. C.; King, A. J. *J. Am. Chem. Soc.* **1936**, *58*, 333−337.
(3) Clark, G. L.; Parker, E. A. *J. Phys. Chem.* **1937**, *41*, 777−786.
(4) Hess, K; Gundermann, J. *Ber.* **1937**, *B70*, 1788−1790.
(5) Legrand, C. *J. Polym. Sci.* **1951**, *7*, 333−339.
(6) Sarko, A.; Southwick, J.; Hayashi, J. *Macromolecules* **1976**, *9*, 857−863.
(7) Trogus, C.; Hess, K. *Z. Phys. Chem. Abt. B* **1931**, *14B*, 387−395.
(8) Davis, W. E.; Barry, A. J.; Peterson, F. C.; King, A. J. *J. Am. Chem. Soc.* **1943**, *65*, 1294−1299.
(9) Loeb, L.; Segal, L. *J. Polym. Sci.* **1955**, *15*, 343−354.
(10) Creely, J. J.; Wade, R. H. *Text. Res. J.* **1975**, *45*, 240−246.

(11) Creely, J. J.; Wade, R. H. *J. Polym. Sci., Polym. Lett. Ed.* **1978**, *16*, 291−295.
(12) Klemm, D.; Philipp, B.; Heinze, U.; Wagenknecht, W. In *Comprehensive Cellulose Chemistry*; Wiley-VCH: New York, 1998; Vol. I, pp 152−154.
(13) Klenkova, N. I. *Zh. Prikl. Khim.* **1967**, *40*, 2191−2208.
(14) da Silva Perez, D.; Montanari, S.; Vignon, M. R. *Biomacromolecules* **2003**, *4*, 1417−1425.
(15) Herrick, F. W. *J. Appl. Polym. Sci., Appl. Polym. Symp.* **1983**, *37*, 993−1023.
(16) Bonner, W. T. US Patent 1,173,336, 1916.
(17) Schleicher, H.; Daniels, C.; Philipp, B. *J. Polym. Sci., Polym. Symp.* **1974**, *47*, 251−260.
(18) Schuerch, C. US Patent 3,282,313, 1966.
(19) Lindberg, K. J.; Stranger-Johannessen US Patent 3,406,006, 1968.
(20) Roldan, L. G. In *Modified Cellulosics*; Rowell, R. M., Young, R. A., Eds.; Academic Press: New York, 1978; pp 303−319.
(21) Roche, E.; Chanzy, H. *Int. J. Biol. Macromol.* **1981**, *3*, 201−206.
(22) Chanzy, H.; Henrissat, B.; Vuong, R.; Revol, J.-F. *Holzforschung* **1986**, *40 Suppl*, 25−30.
(23) Sugiyama, J.; Harada, H.; Saiki, H. *Int. J. Biol. Macromol.* **1987**, *9*, 122−130.
(24) Lewin, M.; Roldan, L. G. *J. Polym. Sci., Part C* **1971**, *36*, 213−229.
(25) Rousselle, M.-A.; Nelson, M. L. *Text. Res. J.* **1976**, *46*, 648−653.
(26) Chanzy, H.; Henrissat, B.; Vincendon, M.; Tanner, S. F.; Belton, P. S. *Carbohydr. Res.* **1987**, *160*, 1−11.
(27) Isogai, A.; Usuda, M.; Kato, T.; Uryu, T.; Atalla, R. H. *Macromolecules* **1989**, *22*, 3168−3172.
(28) Wada, M.; Heux, L.; Isogai, A.; Nishiyama, Y.; Chanzy, H.; Sugiyama, J. *Macromolecules* **2001**, *34*, 1237−1243.
(29) Kono, H.; Erata, T.; Takai, M. *Macromolecules* **2003**, *36*, 3589−3592.
(30) The conformation of the hydroxymethyl group is defined by two letters, the first referring to the torsion angle χ (O5−C5−C6−O6) and the second to the torsion angle χ' (C4−C5−C6−O6). Thus, the ideal *tg* and *gt* conformations would be respectively be defined as sets of two angles (180°, 60°) and (60°, 180°). The glycosidic bond angle τ is defined by (C1−O4−C4). The glycosidic torsion angles Φ and Ψ, which describe the relative orientation of adjacent glucosyl residues in the same chain, are defined by (O5−C1−O1−C4) and (C1−O1−C4−C3), respectively.
(31) Horii, F.; Hirai, A.; Kitamaru, R. *Polym. Bull. (Berlin)* **1983**, *10*, 357−361.
(32) Lee, D. M.; Burnfield, K. E.; Blackwell, J. *Biopolymers* **1984**, *23*, 111−126.
(33) Henrissat, B.; Marchessault, R. H.; Taylor, M. G.; Chanzy, H. *Polym. Commun.* **1987**, *28*, 113−115.
(34) Yatsu, L. Y.; Calamari, T. A., Jr.; Benerito, R. R. *Text. Res. J.* **1986**, *56*, 419−424.
(35) Isogai, A.; Usuda, M. *Mokuzai Gakkaishi* **1992**, *38*, 562−569.
(36) Sugiyama, J.; Persson, J.; Chanzy, H. *Macromolecules* **1991**, *24*, 2461−2466.
(37) Nishiyama, Y.; Kuga, S.; Wada, M.; Okano, T. *Macromolecules* **1997**, *30*, 6395−6397.
(38) Nishiyama, Y.; Langan, P.; Chanzy, H. *J. Am. Chem. Soc.* **2002**, *124*, 9074−9082.
(39) Von der Linden, W.; Dose, V.; Padayachee, J.; Provesky, V. *Phys. Rev. E* **1999**, *59*, 6527−6534.
(40) Nishiyama, Y.; Langan, P. *Fibre Diffr. Rev.* **2000**, *9*, 18−23.
(41) Sheldrick, G. M. *SHELX-97*, a program for the refinement of Single-Crystal Diffraction Data; University of Gottingen: Gottingen, Germany, 1997.
(42) Langan, P.; Nishiyama, Y.; Chanzy, H. *Biomacromolecules* **2001**, *2*, 410−416.
(43) The "parallel-up" and "parallel-down" structures are defined according to the definition of: French, A. D.; Howley, P. D. In *Cellulose and Wood, Chemistry and Technology*; Schuerch, C., Ed.; Wiley: New York, 1989; p 164.
(44) R is calculated from $\sum(|F_o| - |F_c|)/\sum|F_o|$ with $F_o > 4\sigma$, where F_o and F_c are the observed and calculated amplitudes, respectively. $R\omega$ is calculated from $[\sum\omega(F_o^2 - F_c^2)^2/\sum\omega(F_o^2)^2]^{1/2}$, where ω is a weight $(1/\sigma^2)$ applied to each F^2 term in the least-squares refinement. $R\omega$ will be more than twice the size of R.
(45) Hamilton, W. C. *Acta Crystallogr.* **1965**, *18*, 502−510.
(46) Langan, P.; Nishiyama, Y.; Chanzy, H. *J. Am. Chem. Soc.* **1999**, *121*, 9940−9946.
(47) Nishiyama, Y.; Sugiyama, J.; Chanzy, H.; Langan, P. *J. Am. Chem. Soc.* **2003**, 125, 14300−14306.
(48) Gessler, K.; Krausss, N.; Steiner, T.; Betzel, C.; Sandmann, C.; Saenger, W. *Science* **1994**, *266*, 1027−1029.
(49) Raymond, S.; Heyraud, A.; Tran Qui, D.; Kvick, Å; Chanzy, H. *Macromolecules* **1995**, *28*, 2096−2100.
(50) Raymond, S.; Henrissat, B.; Tran Qui, D.; Kvick, Å.; Chanzy, H. *Carbohydr. Res.* **1995**, *277*, 209−229.
(51) Gessler, K.; Krauss, N.; Steiner, T.; Betzel, C.; Sarko, A.; Saenger, W. *J. Am. Chem. Soc.* **1995**, *117*, 11397−11406.
(52) French, A. D.; Johnson, G. P. *Cellulose* **2004**, *11*, 5−22.
(53) Cremer, D.; Pople, J. *J. Am. Chem. Soc.* **1975**, *97*, 1354−1358.
(54) Jeffrey, A. J. *An Introduction to Hydrogen Bonding*; Oxford University Press: New York, 1997.
(55) Jakobsen, R. J.; Brasch, J. W.; Mikawa, Y. *J. Mol. Struct.* **1967**−**1968**, *1*, 309−321.
(56) Jarvis, M. *Nature (London)* **2003**, *426*, 611−612.
(57) Numata, Y.; Kono, H.; Kawano, S.; Erata, T.; Takai, M. *J. Biosci. Bioeng.* **2003**, *96*, 461−466.
(58) Segal, L.; Nelson, M. L. *J. Am. Chem. Soc.* **1954**, *76*, 4626−4630.

MA0485585